Basrah Journal for Engineering Sciences

OPEN ACCESS

Effect of Retained Austenite on the Microstructure and Micro-Hardness of AISI 4330 Low Alloy Steel Using X-Ray Diffraction method

Hadeel K. Abdul Reda [1,*], Haider M. Mohammad [2]

[1] *Department of Mechanical Engineering, College of Engineering, University of Basrah, Basrah, Iraq*
[2] *Department of Material Engineering, College of Engineering, University of Basrah, Basrah, Iraq*
E-mail addresses: engpg.hadeel.kareem@uobasrah.edu.iq , haider.mohammed@uobasrah.edu.iq

Abstract

The mechanical properties of low alloy steel are significantly influenced by retained austenite (RA). Consequently, using the X-Ray diffraction (XRD) measurement method, the retained Austenite volume fractions in AISI4330 alloy steel have been assessed in this article. The specimens underwent heat treatment at various heating temperatures (800 ℃, 900 ℃, 1000 ℃) and cooling rates (Water and Oil). The findings demonstrate that retained Austenite formation rises with rising heating (Austenitizing) temperatures for the same quenching media as well as with rising cooling rates. The specimens were heated to a temperature of 1000 °C and then quenched in water, yielding the highest amount of retained austenite (7.733 wt%), and the lowest amount (1.977 wt%), which was obtained when the specimens were heated to a temperature of 800 °C and quenched in oil. The Vickers method was employed to conduct micro-hardness testing, and the results demonstrate that hardness values are reduced as heating temperatures increase. Optical microscopy was used to investigate the effects of retained austenite on the microstructure. The results show that bainite and/or martensite phases with a small amount of retained austenite dominate the microstructure at low cooling rates, whereas martensite and retained austenite phases dominate the microstructure at higher heating and cooling rates.

Keywords: Martensite, Micro-Hardness, Retained Austenite, X-Ray diffraction

1. Introduction

To process or manufacture steel with the necessary qualities, it is crucial to comprehend which phases of iron and carbon form as a function of temperature and carbon content. Every phase has unique properties, including strength, hardness, and ductility. These characteristics are important while producing steel. Steel begins to generate austenite at temperatures above 725 °C [1]. Due to the fcc crystal structure of austenite, carbon atoms can diffuse into the structure without altering the structure. Because the carbon atoms do not have enough time to diffuse out of the crystal structure when steel is quenched in a media (often water, oil, or gas), martensite develops [1]. Instead of bcc, the trapped carbon atoms lead to the bct crystal structure. The steel is typically heated to the austenitic forming area and then cooled during the manufacturing process. When steel is at room temperature, some austenite is still present. Following this, the steel is frequently heat treated at lower temperatures to permit some of the carbon to diffuse out of the bct martensite. Steel that is created in this way is less hard and more ductile. Any austenite retained is frequently undesirable. To prevent any corresponding deformation and/or loss of fracture toughness in the finished piece, lower amounts of residual austenite are often targeted because it can change into martensite with a nominal 4 percent volume expansion [2]. Retained austenite hence leads to

distortion in the steel, which is undesirable for the majority of precision steel parts. In this article, experimental research is presented to look at how retained austenite affects the microstructure and micro-hardness specimens manufactured of AISI4330 at varied austenitizing temperatures, holding times, and quenching media.

Hiroshi Matsuda et al., 2010 [3], studied the transformation behavior of blocky and lath-shaped retained austenite, to further understand how straining affected mechanical properties. Two different TRIP steel kinds with approximately the same amounts of retained austenite but distinct morphologies were employed. They found that superior ductility and excellent work-hardenability are maintained in a high strain zone in steel containing a significant quantity of lath-shaped retained austenite. The ductility of steel with a lot of blocky retained austenite is low, in contrast. In a low-strain zone, the work hardenability rose sharply to its maximum and then decreased in a high-strain area. Blocky austenite has been discovered to have poor stability concerning martensite transition. While the blocky retained austenite changed into martensite in a low-strain zone, the lath-shaped retained austenite remained until a high-strain region. Lath-shaped retained austenite contained more carbon than blocky retained austenite did. However, the carbon content

alone cannot explain the stability of the retained austenite, which would also be impacted by the altered shape and the ensuing constraint circumstances.

M. A. Jabbar, 2010 [4], discussed how Retained Austenite affects the tensile strength and hardness of AISI 1144, AISI 4140, and AISI 4340. These alloys were heated to temperatures between (750 C and 1000 C), quenched in a variety of quenching media, and then tempered. Tensile strength and hardness were found to be at their highest levels between (825°C and 875°C), and when the volume fraction of retained austenite increased by over 14 percent, these values either fell or stayed the same.

Z.A.Hamza et al., 2015 [5], studied how heat treatment affected some of the mechanical properties of low alloy steel AISI 4340 (nickel-chromium-molybdenum). A series of tests and experiments were conducted on the chosen low alloy steel, starting with chemical analysis, specimen preparation, quenching at various temperatures (750,800,850,900, and 950 °C) in various quenchants, tempering at 350 °C for an hour, and finishing with mechanical tests (hardness, Izod impact, and fatigue) tests. Using data regression software (Lab fit), the models for highly performance media were built up taking mechanical properties into account as a function of heat treatment conditions. The results showed that optimum hardness and fatigue resistance by quenching from (800 to 850 C) and heating for high temperature reached 950 C increased Izod impact strength. Microstructural changes during heating and cooling cycles were the key factor to improve mechanical properties for low alloy steel.

N. M. Abdulkareem & M. A. Jabbar, 2017 [6], determined the volume fraction of austenite retained using the two methods (magnetization and X-ray diffraction) in samples of AISI 4340 low alloy steel after heat treatment under different conditions (temperature, cooling medium, and cooling rate) and compared between the results of both methods. They also examined the samples to find the effect of retained austenite on the microstructure using scanning electron microscopy and optical microscopy. They found that the results obtained from both methods are almost identical. And that the retained austenite formation increases with the increase in the cooling rate and the heating temperature for the same quenching medium, as the maximum amount of it (27.2% by weight) in samples that were heated to 1000°C and quenched in water, while the lowest amount of retained austenite (7.06 wt%) in samples that were heated to 800°C and quenched in the sand. And they found from the results of microscopy and optical examination that the microstructure will consist of bainite and/or martensite and a little austenite retained when the cooling rate is low, while the microstructure will consist of martensite and austenite retained when the cooling rate and heating temperature increase.

M. Morawiec & A. Grajcar 2017 [7], calculated the quantitative analysis and phase determination of the retained austenite after performing an X-ray diffraction assay using the X-pert Highscore Microsoft that includes the Rietveld refinement method for the experimentally thermo-mechanically and rolled steels that have been cooled to room temperature. They found that the microstructure consists of a fine-grained bainitic matrix that includes (bainite-austenite, blocks of martensite, and some retained austenite). They also found

through X-ray diffraction analysis that this includes phases and 14.1% is the volumetric fraction of austenite retained from Rietveld analysis.

Jiri Pechousek et al 2018 [8], calculated the amount of austenite retained in the steel using Mössbauer spectroscopy, and the thickness of the analyzed surface was 20 μm. They compared the results obtained with the results of XRD. It has been concluded that the results obtained from MS are more resistant to the arrangement, preparation, and composition of the sample, and also that this rapid ability to calculate austenite can be used for samples with a diameter of up to 2 cm and more. Also, they found that although the samples contain alloying elements and large amounts of retained austenite, the Mössbauer spectra appear more complex, so the samples must be analyzed more accurately.

Peter I. Christodoulou et al., 2018 [9], treated the properties of the retained austenite using a bainite isothermal transformation in aluminum-containing TRIP700 steel. Quantitative image analysis and optical microscopy were used to verify the evolution of the microstructure, while they used the saturation magnetization method to calculate the amount of austenite retained. They found that the stability of RA and the applied strain amplitude affect the cyclic behavior. Low Cycle Fatigue (LCF) performance is enhanced by less stable RA microstructures, which facilitate cyclic softening and limit the rate of cycle softening at strain amplitudes with comparable elastic and plastic strain components. A shift to cyclic hardening is seen with increasing plastic strain components, and the transition strain rises with increasing RA stability. Due to severe cyclic strain hardening that encourages martensitic transformation, LCF performance suffers. A change from mixed dimple/cleavage to cleavage-type fracture features occurs along with the effect.

Takayuki Yamashita et al., 2019 [10], determined the retained austenite present in low-alloy steels during tensile tests and at low temperatures using neutron diffraction, analyzed phase fraction, phase stresses, and discussed them as the deformation progresses. They found that the role of austenite retained in steel during low-temperature deformation is not direct in strength, but upon transformation to martensite, it improves elongation as well as increases the rate of work hardening through work hardening of martensite and increases the phase fraction of martensite.

2. X-ray diffraction measurement principles for retained austenite

The Society of Automotive Engineers presents a thorough explanation of a retained austenite measurement using X-ray diffraction. Since steel contains crystalline phases like ferrite, martensite, and austenite, X-irradiating a steel sample results in a distinct X-ray diffraction pattern for each crystalline phase. X-ray diffraction patterns will also be produced by the steel's carbide phases. Since the total integrated intensity of all diffraction peaks for each phase is proportional to the volume fraction of that phase, it is possible to calculate the relative volume fractions of ferrite and austenite for a randomly oriented sample using X-ray diffraction patterns. The integrated intensity from any one diffraction peak (hkl) crystalline plane is

proportional to the volume fraction of that phase of the crystalline phase or grains of each phase are randomly oriented:

$$I_\alpha^{hkl} = KR_\alpha^{hkl}V_\alpha/2\mu \qquad (1)$$

Where

$$K = (I_0 e^4/m^2 c^4) * (\lambda_A^3/32\pi r) \qquad (2)$$

And

$$R_\alpha^{hkl} = \frac{1(|F|^2 pLPe^{-2M})}{v^2} \qquad (3)$$

$$Lp = (1 + \cos^2 2\,\theta)/(\sin^2 \theta \cos \theta) \qquad (4)$$

For normal diffract metric analysis but becomes:

$$Lp = (1 + \cos \theta^2\, 2\alpha \cos^2 2\,\theta)/(\sin^2 \theta \cos \theta)(1 + \cos^2 2\,\alpha) \qquad (5)$$

When a monochromator is used.

If the diffraction by monochromator occurs in a plane perpendicular to the plane of sample diffraction then.

$$Lp = (\cos^2 2\,\alpha + \cos^2 2\,\theta)/\sin^2 \theta \cos(1 + \cos^2 2\,\alpha) \qquad (6)$$

where

$$M = B(\sin \theta\,/\lambda)^2 \qquad (7)$$

And

$$B = 8\pi^3 (\mu_s)^2 \qquad (8)$$

Therefore, the integrated intensity from the (hkl) planes of the ferrite phase is expressed as follows if the sample contained ferrite and/or martensite (α), austenite (γ), and no carbides:

$$I_\alpha^{hkl} = KR_\alpha^{hkl}V_\alpha/2\mu \qquad (9)$$

Applying a similar equation to austenite leads to:

$$I_\gamma^{hkl} = KR_\gamma^{hkl}V_\gamma/2\mu \qquad (10)$$

The following can be written for any pair of austenite and ferrite:

$$\frac{I_\alpha^{hkl}}{I_\gamma^{hkl}} = \left[\left(\frac{R_\alpha^{hkl}}{R_\gamma^{hkl}}\right)\left(\frac{V_\alpha}{V_\gamma}\right)\right] \qquad (11)$$

But $V_\alpha + V_\gamma = 1$ $\qquad (12)$

Each ratio of observed integrated intensity to R-value can be added together for a variety of ferrite and austenite peaks [11].

$$V_\gamma = \left[\left(\frac{I_\gamma}{R_\gamma}\right)/\left\{\left(\frac{I_\alpha}{R_\alpha}\right) + \left(\frac{I_\gamma}{R_\gamma}\right)\right\}\right] \qquad (13)$$

For numerous ferrite and austenite peaks, each ratio of measured integrated intensity to R-value can be summed.

$$V_\gamma = \left[\frac{1}{q}\sum_{j=1}^q \left(\frac{I_{\gamma j}}{R_{\gamma j}}\right)/\left\{\left(\frac{1}{p}\sum_{i=1}^p \frac{I_{\alpha i}}{R_{\alpha i}}\right) + \left(\frac{1}{q}\sum_{j=1}^q \frac{I_{\gamma j}}{R_{\gamma j}}\right)\right\}\right] \qquad (14)$$

If carbides are present:

$$V_\alpha + V_\gamma + V_c = 1 \qquad (15)$$

For the ratio of the measured ferrite and austenite integrated intensity to R - volume, the volume fraction of austenite is:

$$V_\gamma = \left[(1 - V_C)\left(\frac{I_\gamma}{R_\gamma}\right)/\left\{\left(\frac{I_\alpha}{R_\alpha}\right) + \left(\frac{I_\gamma}{R_\gamma}\right)\right\}\right] \qquad (16)$$

The ratio of measured integrated intensities to R-value for various ferrite and austenite peaks can be added up as follows:

$$V_\gamma = \left[(1 - V_C)\left(\frac{1}{q}\sum_{j=1}^q \frac{I_{\gamma j}}{R_{\gamma j}}\right)/\left\{\left(\frac{1}{q}\sum_{i=1}^q \frac{I_{\alpha i}}{R_{\alpha i}}\right) + \left(\frac{1}{q}\sum_{j=1}^q \frac{I_{\gamma j}}{R_{\gamma j}}\right)\right\}\right] \qquad (17)$$

The volume fraction of carbides (VC) should be determined by the chemical extraction metallographic method [11]. In this paper, the phase composition is considered to have consisted of martensite and austenite only.

3. Experimental Work

Finding a precise correlation between retained austenite and factors affecting it, as well as the impact of retained austenite on mechanical properties, is challenging. Several experimental works need to be made to address this problem.

To verify their findings, a chemical composition test was performed following ASTM A751 standard [12] and the required material (AISI4330) was acquired from (ONLINE METAL.COM TM) company. The chemical composition of the specimens is presented in Table (1).

Table (1) AISI 4330 Low Alloy Steel Chemical Analysis

Element	Measured Values Wt%	Standard Values Wt % [33]
C	0.293	0.20-0.30
Si	0.279	≤0.80
Mn	0.91	≤1.00
P	0.0030	0.025
S	0.0020	0.025
Cr	0.55	0.40-0.60
Mo	0.41	0.30-0.50
Ni	1.07	1.00-1.50
Fe	Balance	Balance

The austenite stabilized elements for AISI4330 alloy steel are 1.07wt% nickel and 0.91wt% manganese, whereas the ferrite stabilized elements are 0.55wt% chromium, 0.41wt% molybdenum, and 0.0020wt% silicon. Such steel will have a martensite or bainite microstructure with a significant amount of residual austenite. Because retained austenite is present, the strength and hardness values for this steel will either decrease or remain unchanged as the critical rate of cooling decreases and the heating temperature rises.

3.1. Machining and preparation of specimens

Following ASTM A370 [13] and ASTM E975 [14] standards, 40 specimens were prepared. Following the steps below, these specimens were machined in a workshop:

1. The specimens were brought as long normalizing bar.
2. The bar was precisely cut to the required dimensions of (1 cm) thickness by (5 cm) diameter for specimens for optical microscopy, X-ray diffraction, and micro-hardness, as shown in Figure (1).
3. After applying heat treatment procedures at various temperatures and using various quenching media, a fine grinding machine was utilized to smooth the surfaces of the specimens.
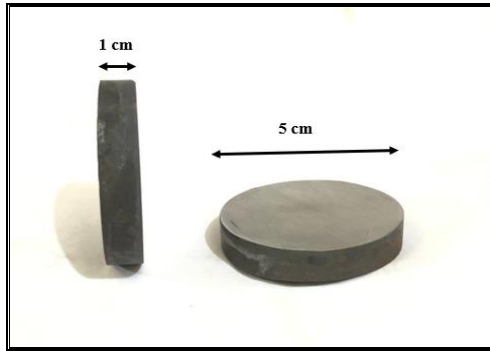
Fig.1 Samples dimensions

3.2. Processes for Heat Treatment, Quenching, and Tempering

Hardening: The first step: The samples are heated to a temperature between (800 ℃, 900 ℃, and 1000 ℃) by using an electrical furnace (HYSC) with a temperature range of 0 to 1100 degrees Celsius and a digital temperature measuring and controlling device.

The second step: Involves maintaining the samples at a specific temperature of (60min).

The third step: Quenching the samples in different cooling media (Oil and Water) to obtain a distinct cooling rate that results in different mechanical properties [15].

Tempering: The quenching treatment frequently results in steel that is excessively hard and brittle for most practical applications. For these reasons, tempering was used to harden steel to lessen brittleness, increase ductility and toughness, and relieve stresses in steel structures. In the current study, the specimens were heated using the same electrical furnace to 250 ℃, held there for a (90min), and then progressively cooled inside the furnace [15].

3.3. Micro-Hardness Test

A diamond indenter with a defined geometry is impressed into the test specimen's surface with a known applied force (often referred to as a "load" or "test load") of 1 to 1000 gf during micro-indentation hardness testing (MHT). Such a test has historically been referred to as "microhardness." Based on measurements of the indent made on the test specimen's surface, the hardness value is calculated [16].

This test was conducted following the ASTM E92 standard [17] using a Chinese-made Microhardness Tester with a 100-400x magnification force. To determine a precise and reliable number for each sample, seven values were calculated. The arithmetic mean was then calculated.

3.4. Optical Microscopic Test

The optical microscopic (Olympus type, Japan-made) used for this test was used to display the microstructure contained. The specimens were manufactured using a grinding and polishing device before the microscopic examination (UNIPOL-820). After that, etching is done using an etching liquid that has been manufactured following ASTM E407 [18] (4g HNO3 with 100mg ethanol). After ten seconds in this liquid, the specimen is submerged in distilled water. microscopic examination was done carefully using a magnification of (x400).

4. Results and Discussion

The data from the XRD for retained austenite are summarized in Table (2). Note that all AISI4330 used specimens were tempered up to 250 ˚C before heat treatment. With increasing heating (austenitizing) temperatures for the same quenching medium, retained austenite production increases. This is because as the temperature rises and the carbon content increases, it forms a part of the crystal structure and causes some or all of the carbides to dissolve, resulting in a high content of RA fractions [19].

The largest RA fractions are attained when using water as the quenching medium, whilst the lowest ones come from quenching with oil. It can also be observed that RA fractions rise with increasing cooling rates. This is because an increase in cooling rate (rapid quenching) will result in less time for RA to change into martensite and a rise in RA fractions.

Table (2) Summary of the XRD data for retained austenite.

Heating temperature °C	Quenching medium	RA fraction calculated value wt%
800	Water	2.324
	Oil	1.977
900	Water	4.093
	Oil	2.87
1000	Water	7.733
	Oil	5.246

It is clear from Figure (2) that the formation of Retained Austenite increases with an increase in heating (Austenizing) temperature for the same cooling medium. This is because when the heating temperature increases, some (or all) of the carbides during heating dissolve, increasing carbon content and causing it to become a part of the crystal structure, due to the large content of retained austenite fractions.

Figure 3 show how retained austenite fractions affect micro-hardness, which is calculated using Vickers hardness (VH). The findings indicate that an increase in retained austenite fraction is causing a decrease in hardness due to the presence of a soft and ductile austenite phase. It is also possible to see how the cooling rate affects hardness since rapid quenching (high cooling rate) increases the likelihood of martensite formation while maintaining the same heating temperature [20].
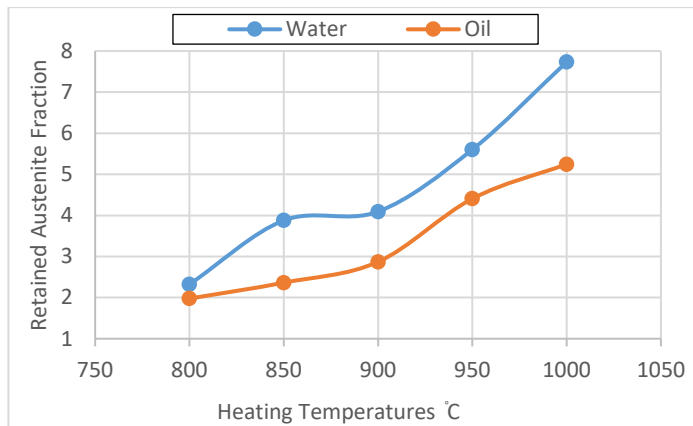
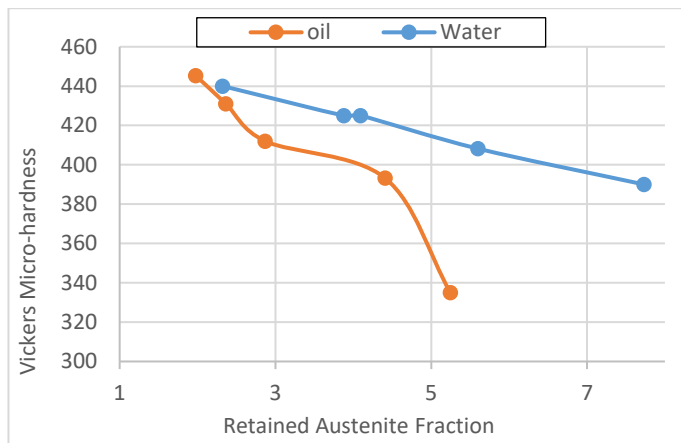Fig. 2 Retained Austenite Fractions measured by XRD method Vs Heating Temperatures.

Fig. 3 Vickers Micro-Hardness Vs Retained austenite fractions.

Fig.4 Microstructure of specimens heating to 800˚C, (A) water quenched while (B) oil quenched.

Fig.5 Microstructure of specimens heating to 1000˚C, (A) water quenched while (B) oil quenched.

The microstructure of a sample is depicted in Figure (4-A) after it has been heated to 800 °C for 60 minutes, quenched in water, and then tempered at 250 °C for 90 minutes. The specimen's structure is formed to consist of retained Austenite (Black areas) and lath Martensite (needle-shape). Figure (4-B) shows a sample's microstructure after it was subjected to heat to 800 °C for 60 minutes, cooled in oil, then tempered at 250 °C for 90 minutes. Bainite, retained Austenite, and needle-shaped Martensite were found to be present in the specimen's lath structure (Black areas).

Figure (5-A) shows the microstructure of a sample after heating to 1000 °C for 60 minutes, quenching in water, and then tempering at 250 °C for 90 minutes. It was found that the specimen contained Retained Austenite (black areas) and a Martensite (plate shape). Figure (5-B) shows the microstructure of a sample after heating to 1000 °C for 60 minutes, quenching in oil, and then tempering at 250 °C for 90 minutes. It was found that the specimen had a coarse Martensite structure (plate-shaped) and that Retained Austenite (black area).
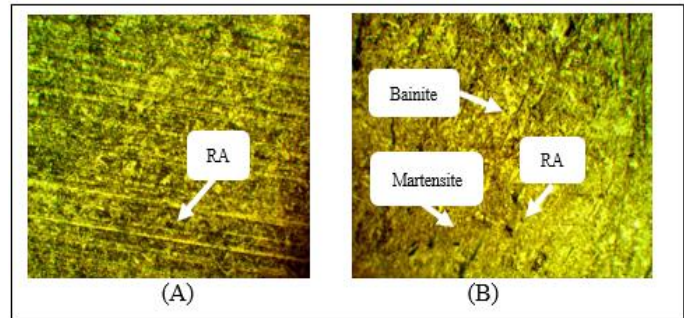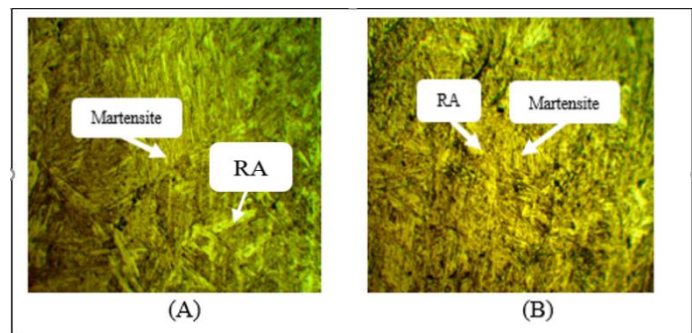
4. Conclusions

The following list of conclusions best captures the findings of this study:

1. Low alloy steel's hardness and microstructure are affected by the existence of retained austenite.
2. The hardness decreases with austenitizing temperature and retained austenite fractions increase. In addition, Hardness increased with the cooling rate, increasing.
3. After quenching in both water and oil, the specimen's microstructure consisted of lath Martensite and retained Austenite.
4. The preserved austenite content, martensite characteristics (such as the sizes and shapes), and often carbide forms are the main microstructural parameters that are affected on the hardness of heat-treated low alloy steel.

5. Nomenclature

Symbol	Description
I_α^{hkl}	The integrated intensity per angular diffraction peak (hkl) in the α – phase.
I_0	The intensity of the incident beam.
μ	The linear absorption coefficient for the steel.
e, m	The charge and mass of the electron respectively.
r	The radius of the diffractometer.
C	The velocity of light.
λ	The wavelength of incident radiation.

A	The cross-sectional area of the incident beam.
v	The volume of the unit cell.
$\lvert f \rvert^2$	The structure factor times its complex conjugate.
P	The multiplicity factor of the (hkl) reflection.
θ	Bragg angle.
Lp	The Lorrents – polarization factor.
2α	The diffraction angle of the monochromator crystal.
e^{-2M}	The Debye-Waller or temperature factor which is a function of θ.
μ_s	The mean square displacements of the atoms from their mean position in a direction perpendicular to the diffraction plane.
V_α	The volume of the α – plane.
K	A constant which is dependent upon the selection of instrumentation geometry and radiation but independent of the nature of the sample.
R	The parameter that is proportional to the theoretically integrated intensity.
TRIP	Transformation Induced Plasticity
bct	Body-Centered Tetragonal

References

[1] H. Chandler, Metallurgy for the Non-Metallurgist, ASM International (1998).

[2] N. Pappas, T.R. Watkins, O.B. Cavin, R.A. Jaramillo, G.M. Ludtka, Retained Austenite in SAE 52100 Steel Post Magnetic Processing and Heat Treatment, Proceedings on Materials Processing under the Influence of External Fields, Edited by Q. Han, G. M. Ludtka and Q. Zhai, The Minerals, Metals & Materials Society (2007) 37–42.

[3] A. N. Vasilakos, J. Ohlert, K. Giasla, G. N. Haidemenopoulos, and W. Bleck, "Low-alloy TRIP steels: A correlation between mechanical properties and the retained austenite stability," Steel Res., vol. 73, no. 6–7, pp. 249–252, 2002, doi: 10.1002/srin.200200204.

[4] M. A. Jabbar, " Effect of Retained Austenite on Tensile Strength and Hardness of Low Alloy Steels Using Artificial Neural Networks", University of Basra, Department of Mechanical Engineering , PP. 1-75 , 2010.

[5] Z.A.Hamza, H.M.Moammed, M.A. Jabbar, "Effect of Quenching and Tempering Treatments on Impact Strength and Fatigue Life of AISI 4340, " University of Basra, Department of Mechanical Engineering , pp. 2075-9746, 2015.

[6] H. Matsuda, H. Noro, Y. Nagataki, and Y. Hosoya, "Effect of retained austenite stability on mechanical properties of 590MPa grade TRIP sheet steels," Mater. Sci. Forum, vol. 638–642, pp. 3374–3379, 2010, DOI: 10.4028/www.scientific.net/MSF.638-642.3374.

[7] L. Zhao, N. H. Van Dijk, E. Brück, J. Sietsma, and S. Van Der Zwaag, "Magnetic and X-ray diffraction measurements for the determination of retained austenite in TRIP steels," Mater. Sci. Eng. A, vol. 313, no. 1–2, pp. 145–152, 2001, DOI: 10.1016/S0921-5093(01)00965-0.

[8] J. Pechousek, L. Kouril, P. Novak, J. Kaslik, and J. Navarik, "Austenitemeter – Mössbauer spectrometer for rapid determination of residual austenite in steels," Meas. J. Int. Meas. Confed., vol. 131, pp. 671–676, 2019, doi: 10.1016/j.measurement.2018.09.028.

[9] K. K. Wang, Z. L. Tan, G. H. Gao, X. L. Gui, and B. Z. Bai, "Effect of retained austenite stability on mechanical properties of bainitic rail steel," Adv. Mater. Res., vol. 1004–1005, pp. 198–202, 2014, DOI: 10.4028/www.scientific.net/AMR.1004-1005.198.

[10] M. Morawiec and A. Grajcar, "Some aspects of the determination of retained austenite using the Rietveld refinement," J. Achieve. Mater. Manuf. Eng., vol. 80, no. 1, pp. 11–17, 2017, DOI: 10.5604/01.3001.0010.1442.

[11] ASTM , "Standard practice for x – ray determination of retained austenite is steel with near random crystallographic orientation" , Annual Book of ASTM standard E975 – 3, ASTM International , 2007.

[12] ASTM , "standard test methods, practices, terminology for chemical analysis of steel products" , Annual Book of ASTM standard A751 – 01, ASTM International , 2001.

[13] ASTM, "standard test methods and definition for mechanical testing of steel products" , Annual Book of ASTM standard A370 – 02, ASTM International , 2002.

[14] ASTM , "Standard practice for x – ray determination of retained austenite is steel with near random crystallographic orientation" , Annual Book of ASTM standard E975 – 3, ASTM International , 2007.

[15] T. Materials, "The Materials Information Company," Technology, vol. 2, p. 3470, 2001, DOI: 10.1016/S0026-0576(03)90166-8.

[16] R. P. Division and N. Delhi, "W W W En Te Ch No L Og Y . W En Te Ch No Og," 1980.

[17] ASTM Standard E92-82, "ASTM E92-82 Standard Test Method for Vickers Hardness of Metallic Materials," Annu. B. ASTM Stand. 4, vol. 82, no. Reapproved, pp. 1–27, 1997.

[18] ASTM E 407-99, "E407-07: Standard Practice for Microetching Metals and Alloys," ASTM Int. West Conshohocken, PA, pp. 1–21, 1999.

[19] Joseph Lucas, "Re magnetization of Magnetos", Lucas Quality Equipment, section D-6, Vol.2, PP.1-8, 1952.

[20] ASM Handbook , "Heat treating" , American Society for Metals , Vol.4, Metals Park, Ohio, USA, 2002.